University of Groningen

Molecular dynamics simulation of the transport of small molecules across a polymer membrane

Sok, R. M.; Berendsen, H. J. C.; van Gunsteren, W. F.

Link to publication in University of Groningen/UMCG research database

Molecular dynamics simulation of the transport of small molecules across a polymer membrane

R. M. Sok, H. J. C. Berendsen, and W. F. van Gunsteren

Molecular dynamics simulation of the transport of small molecules across a polymer membrane

R. M. Sok and H. J. C. Berendsen
Laboratory of Biophysical Chemistry, University of Groningen, Nijenborgh 4,
9747 AG Groningen, The Netherlands

W. F. van Gunsteren
Laboratory of Physical Chemistry, ETH-Zentrum, CH-8092 Zurich, Switzerland

The transport of small molecules through a polymer membrane is modeled using the computer simulation technique of molecular dynamics (MD). The transport coefficient is derived from a combination of the excess free energy and the diffusion constant. Both properties are derived from MD simulations, applied to helium and methane in polydimethylsiloxane (PDMS). The diffusional process appears to have the character of a jump diffusion for methane and less so for helium. Jumps are allowed by fluctuations of the size and shape of holes. Experimental diffusion constants are well reproduced. The excess free energies, determined by a particle insertion method, are lower by 5–7 kJ/mol than experimental values. It is shown that, as a result of a higher solubility, methane has a higher permeability constant than helium, despite its lower diffusion constant.

I. INTRODUCTION

The practical applications of selective gas permeation through polymer membranes has generated large interest in theoretical methods to study the underlying molecular mechanisms. Quantitative predictions of permeability and selectivity open the prospect to develop tools for the design of membranes with predefined properties. Molecular dynamics simulations are the appropriate tool to study diffusion processes; they have been used to study diffusion in polyethylene[1-5] or more recently in polypropylene.[6] However, diffusion alone does not describe the transport process across a membrane because the solubility of the permeant molecule in the membrane is a determining factor as well.

The solubility-diffusion mechanism postulates that permeation is controlled by diffusion of the permeant gas in the membrane which is assumed to be in thermodynamic solution equilibrium with the gas at the interfaces. Thus the permeability coefficient P, defined by the ratio between the flux J of the permeant species and its concentration gradient over the membrane of thickness d

$$J = P \frac{\Delta c}{d} \qquad (1)$$

is given by the product of the diffusion coefficient D and a solubility factor S

$$P = DS \qquad (2)$$

Both D and S can be calculated from molecular dynamics simulations. Here we report a series of simulations to calculate both D and S for the permeation of He and CH_4 through polydimethylsiloxane (PDMS). This system shows the interesting feature that the diffusion coefficient of He is much larger than that of CH_4, but the permeability coefficient is smaller. If the simulation can describe this feature then we are one step closer to the final goal of describing the complete process of permeation based only on chemical structure and interaction parameters.

We shall also analyze the type of diffusional process. In case the process has the character of a jump diffusion, we shall investigate if the activated particle occasionally forces itself through the (static) barriers or if the thermal motion of the polymer network facilitates the jump of the penetrant. These questions will be investigated by closely studying the dynamics of the holes in the polymer during one of these jumps.

The polymer used in our simulation models polydimethylsiloxane (PDMS). This is a more complex and realistic model than the commonly used polyethylene (PE). PDMS is in two ways very different from PE: the presence of methyl side groups, and the difference in the equilibrium value and flexibility of adjacent bond angles Si–O–Si and O–Si–O (see Table I). In an all-*trans* configuration PDMS closes upon itself after about 11 units (Fig. 1). This difference in bond angle makes PDMS almost always amorphous, in contrast to PE. Therefore simulations for PDMS are expected to be more realistic than those for PE, because the presence of crystallites makes the interpretation of experimental data and comparison with simulations less reliable for the latter. Some physical properties of PDMS are listed in Table II.

In Sec. II we summarize the solubility-diffusion mechanism. Section III describes details of the model and the methods used, including the nontrivial generation of the initial polymer matrix. In Sec. IV the results of both the diffusion and solubility simulations are reported, followed by a comparison with experiments and discussion of the results to elucidate the mechanism of diffusion in Sec. V.

II. THEORY

We consider an isothermal homogeneous stationary membrane in which particles are dissolved with a local concentration $c(r)$. The particle flux **J** is assumed to behave in the regime of a linear irreversible process with the gradient of

TABLE I. Simulation parameters.

Bonds	l(nm)			
Si–O	0.160			
Si–CH₃	0.188			

Angles	k_θ (kJ mol⁻¹ rad⁻²)	θ_0		
Si–O–Si	118.4	144.0		
O–Si–O	791.2	109.5		
O–Si–CH₃	418.4	109.5		
CH₃–Si–CH₃	418.4	109.5		

Dihedrals	k_φ (kJ mol⁻¹ rad⁻²)	n	δ	
CH₃–Si–O–Si	3.77	3	0	
Si–O–Si–CH₃	3.77	3	0	
Si–O–Si–O	3.77	3	0	
O–Si–O–Si	3.77	3	0	

Nonbonded	ϵ (kJ/mol)	σ (nm)	q	m
Si	2.4480	0.3385	0.3	28.080
O	0.8493	0.2955	− 0.3	15.999
CH₃	0.7532	0.3786	0.0	15.035
CH₄	1.2466	0.3733	0.0	16.043
He	0.0850	0.2580	0.0	4.0026
$r_{\rm LJ}$	1.0 (nm)			
$r_{\rm coulomb}$	1.1 (nm)			

the chemical potential as the driving force. The flux is given by

$$J(r) = c(r)v(r) \qquad (3)$$

where $v(r)$ is the average velocity of the dissolved particles. In the linear regime $v(r)$ can be written as

$$v(r) = \frac{1}{\zeta} F_{\rm th} = -\frac{1}{\zeta} \nabla \mu(r), \qquad (4)$$

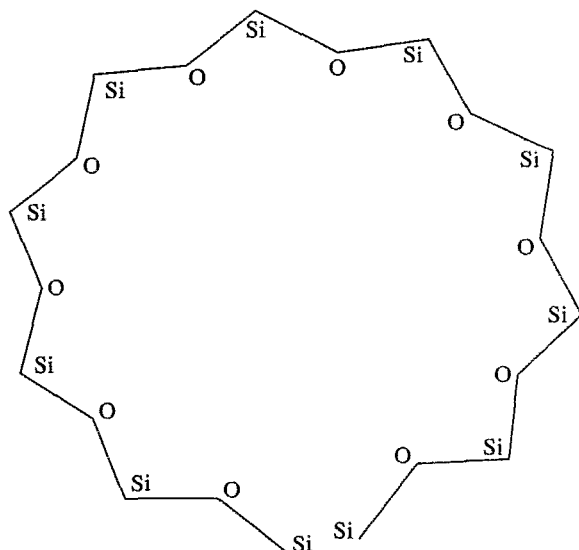where $F_{\rm th}$ is the thermodynamic force, ζ a friction coeffi-

FIG. 1. All-trans configuration of PDMS.

TABLE II. Some characteristics of polydimethylsiloxane (PDMS) (Ref. 7).

Repeating unit	$\begin{array}{c} \mathrm{CH_3} \\ | \\ \mathrm{—Si—O—} \\ | \\ \mathrm{CH_3} \end{array}$
MW repeating unit	74.15
Glass transition temperature	− 128 °C
Melting temperature	− 40 °C
Average density	0.95g cm⁻³

cient, and μ the chemical potential of the dissolved particles. The latter can be written as

$$\mu(r) = \mu^0 + RT \ln c(r) + \mu_{\rm ex}(r), \qquad (5)$$

in which μ^0 is the standard chemical potential of the ideal gas phase based on concentration, c is the local concentration and $\mu_{\rm ex}(r)$ is the excess chemical potential of the dissolved species with respect to the ideal gas state. Equations (3), (4), and (5) give

$$J(r) = \frac{-RT}{\zeta} \nabla c(r) - \frac{c(r)}{\zeta} \nabla \mu_{\rm ex}(r). \qquad (6)$$

Equating RT/ζ with the diffusion coefficient D, Eq. (6) can be written as

$$\begin{aligned} J(r) = & -D \exp[-\mu_{\rm ex}(r)/RT] \\ & \times \nabla\{c(r) \exp[\mu_{\rm ex}(r)/RT]\}. \end{aligned} \qquad (7)$$

Equation (7) is still general. We now consider a membrane with thickness d in the x direction and infinite dimensions in the yz plane. The interfaces at $x = 0$ and $x = d$ are in contact with concentrations c_1 and c_2 ($\Delta c = c_2 - c_1$), and we assume that an ideal gas phase is in equilibrium across both interfaces. Hence μ is continuous at the interfaces. Furthermore, $\mu_{\rm ex}$ is assumed to be constant throughout the homogeneous membrane. This implies that any concentration dependence of $\mu_{\rm ex}$ is neglected. Thus

$$\mu^0 + RT \ln c_1 = \mu^0 + RT \ln c(0) + \mu_{\rm ex} \qquad (8)$$

or

$$c(0) = c_1 \exp(-\mu_{\rm ex}/RT). \qquad (9)$$

Similarly,

$$c(d) = c_2 \exp(-\mu_{\rm ex}/RT). \qquad (10)$$

If $J(r)$ is stationary then $c(x)$ is a linear function of x and the gradient in Eq. (7) is equal to $[c(d) - c(0)]/d$. Equation (7) now reduces to

$$J = -DS \frac{\Delta c}{d} \qquad (11)$$

with

$$S = \exp(-\mu_{\rm ex}/RT). \qquad (12)$$

Equation (11) expresses the solubility-diffusion mechanism. All the information needed from the simulations is the diffusion constant D in the bulk polymer (so it is not necessary to explicitly simulate a membrane) and the excess

chemical potential μ_{ex} of the particles in the membrane compared to the ideal gas phase.

III. MODEL AND SIMULATION DETAILS

A. Description of the simulated system

The simulated system consists of 5 chains of 30 monomer units $[-Si(CH_3)_2-O-]$ and one penetrant particle (either CH_4 or He), all subject to rectangular periodic boundary conditions. In order to reduce end group effects, the end groups of the chains are taken to be methyl groups. No cross links have been inserted.

The CH_3 side groups of the chain and the diffusant CH_4 are modeled as united atoms using the normal GROMOS[8] potential energy functions. Bond lengths are constrained using the SHAKE[9] method. Bond angle vibrations are treated by a harmonic potential

$$V(\theta) = \tfrac{1}{2}k_\theta(\theta - \theta_0)^2 \qquad (13)$$

and the dihedral rotations are described by a potential function of the form

$$V(\varphi) = k_\varphi[1 + \cos(n\varphi - \delta)], \qquad (14)$$

where θ_0 is the equilibrium angle, k_θ and k_φ are the force constants, δ a phase shift, and n the multiplicity factor. The nonbonded interactions are represented by a Lennard-Jones 12–6 potential

$$V(r) = 4\epsilon[(\sigma/r)^{12} - (\sigma/r)^6]. \qquad (15)$$

The electrostatic interactions are given by

$$V(r) = \frac{q_i q_j}{4\pi\epsilon_0 r}. \qquad (16)$$

Lennard-Jones forces were considered for $r < r_{LJ}$ and Coulomb forces for $r < R_{coulomb}$. The latter were computed every time step for $r < r_{LJ}$ and once every ten time steps for $r_{LJ} < r < R_{coulomb}$. The parameters used in the simulation are listed in Table I.

The equations of motion for the 606 (united) atoms are solved using the leap-frog[10] algorithm with a time step of 5 fs. Simulations were carried out under NPT conditions using the weak coupling scheme to a temperature and pressure bath ($T = 300$ K, $P = 1$ atm) with coupling constants of 0.1 and 0.5 ps, respectively.[11]

B. Initial configuration

The specific properties of amorphous polymers prevent the usual preparation of a starting configuration, i.e., melting an idealized structure. Because the correlation lengths and times of the equilibration processes in polymers are some orders of magnitude larger than are feasible with MD, we need some other way of preparing a starting sample. A commonly used method is based on a self-avoiding random walk.[12] In this method a chain is built up site by site. The position of the next site is chosen on the basis of the position of the previous site, using a given bond length and angle and a randomly chosen dihedral angle. This site position is then either accepted or rejected with a Monte Carlo-type criterion. The disadvantage of this method is that at higher densi-

ties the acceptance rate of adding another site is practically zero.

The method we have employed to avoid this problem is based on MD rather than MC and uses *soft-core potentials*. One starts with a very dilute system of several chains subject to the normal periodic boundary conditions which interact through the normal bonded forces. The nonbonded forces are not van der Waals like, but are represented by a soft core repulsive potential

$$V(r) = V_{max}[1 - (r/r_{SC})^2]^2 \quad r < r_{SC}$$
$$= 0 \quad r \geqslant r_{SC}. \qquad (17)$$

In the preparation phase V_{max} is set such that molecules are able to move through each other. Though unphysical it prevents the chains from getting trapped. Every MD step the size of the simulation box is decreased by a small amount until the correct density is reached. (In practice one should even go to a slightly higher density to allow for pressure relaxation in the first normal MD steps.) At this time an energy minimization is performed with the normal Lennard-Jones-type nonbonded interaction to relieve the excess stress in the system, after which normal molecular dynamics steps can be done. When following this procedure the system relaxes within 20 ps from a density of 1 to 0.95 g/cm^3, which is about the experimental density of PDMS with chain lengths of 30 units.

C. Diffusion constant, chemical potential, and accessible volume

The diffusion constants are calculated from the root mean square displacement of the particles averaged over all possible time origins

$$D = \lim_{t \to \infty} \frac{1}{6t} \langle [\mathbf{r}_t - \mathbf{r}_0]^2 \rangle. \qquad (18)$$

The chemical potential is calculated using the Widom particle insertion method.[13] In this method one inserts a virtual particle at a random position in the sample and calculates its interaction energy E. The thermodynamic potential is then calculated using

$$\mu_{ex} = -RT \ln\langle\exp(-E/kT)\rangle, \qquad (19)$$

where the angular brackets denote an ensemble average. We combined the basic particle insertion method with an accessible volume map (which will be discussed below) to improve the efficiency.[14]

In simulations of PE one often defines a quantity called the "free volume fraction" v_f of a polymer system as

$$v_f = \frac{v_{tot} - v_c}{v_{tot}}, \qquad (20)$$

where v_{tot} is the total volume and v_c is the volume occupied by the polymer chains, based on an atomic radius of $\sigma_{polymer}/2$ ($\sigma_{polymer}$ being the Lennard-Jones diameter of the polymer). This quantity can only be applied to PE-type models. We therefore use the "accessible volume fraction" of a polymer system to a certain diffusant, which is the volume in the system that is accessible to the penetrant. This quantity is effectively the volume not occupied by the polymer
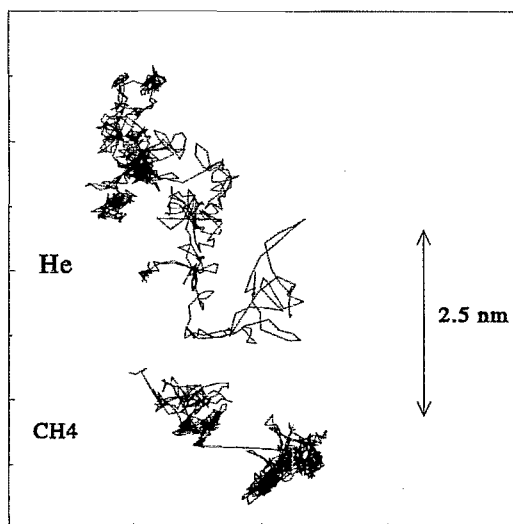
FIG. 2. Trajectories of a CH_4 (during 250 ps) and a He(150 ps) particle in PDMS. The arrow indicates the box size.

FIG. 4. Size of the hole containing the penetrant particle (CH_4) during 5 ps. The arrow corresponds to the time of the jump.

chain, based on a radius $(\sigma_{polymer} + \sigma_{penetrant})/2$. It will therefore always be smaller than the free volume fraction and it will depend on the size of the penetrant. In practice, we calculated this accessible volume fraction on a grid of $100 \times 100 \times 100$ (the distance between gridpoints is about 0.025 nm). With this three dimensional grid one can study the penetrant-accessible "holes" in the system. (A hole is defined as the set of grid points which are directly connected; no diagonal connections). If we follow these holes in time we are able to study the dynamics of the accessible volume.

IV. RESULTS

Figure 2 shows projections of the trajectories of two separate runs: a 250 ps run with a CH_4 and a 150 ps run with a
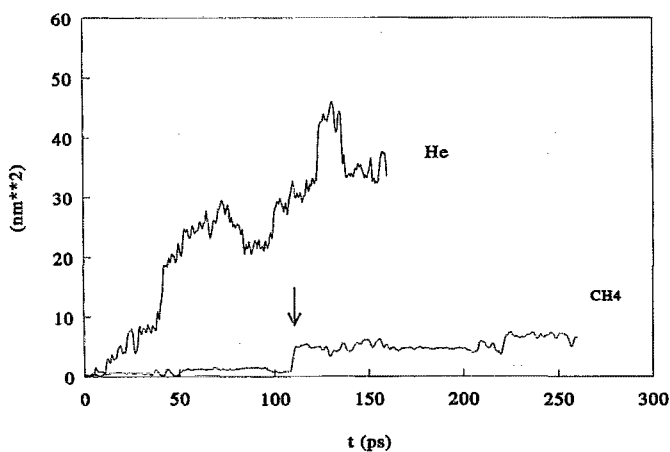

FIG. 3. Squared radial displacements of CH_4 and He. The arrow indicates the jump which is examined in Figs. 4 and 5. The data shown are running averages (ten points) to reduce the noise level.
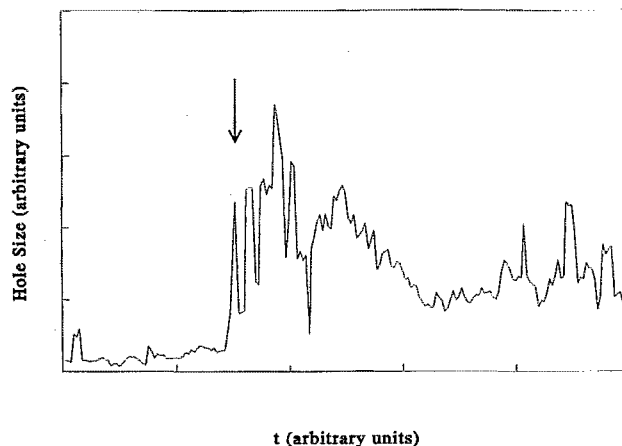
He particle in the bulk polymer (not shown). A good measure of the diffusion process is the squared radial displacement

$$[\Delta r(t)]^2 = (\mathbf{r}_t - \mathbf{r}_0)^2 \tag{21}$$

of these diffusing particles (Fig. 3). To study the jumps we examined one jump of CH_4 more closely. During this jump (indicated by the arrow in Fig. 3) the size of the hole in which the penetrant molecule is situated is plotted in Fig. 4. The size of the hole increases just before the jump is made. To clarify this we have made a projection of the holes during that jump (Fig. 5) and it is clear that two holes are connecting before the jump occurs. So a channel is opened for the particle to move through. This opening of the channel is necessary for a particle to move from one hole to the other, as is shown in a simulation where the membrane is frozen (position restrained). The penetrants are now not able to move to another hole within 250 ps; they can only "rattle" in their cage (Fig. 6).

The diffusion constants calculated with the mean squared displacements [Eq. (18)] from these one-particle trajectories are fairly close to the experimental data [$2.1(\pm 0.8) \times 10^{-9}$ m²/s for CH_4 and $18(\pm 2) \times 10^{-9}$ m²/s for He]. The diffusion constant for CH_4 has been calculated from two separate runs of 250 ps to get the desired accuracy. With these data the fit through the mean squared displacement curve of CH_4 (Fig. 7) gives a diffusion constant with an error in the order of 40%. For He, one run of 150 ps was sufficient.

The chemical potential calculated with Eq. (19) is $-6.3(\pm 0.2)$ kJ/mol for CH_4 and $+3.8(\pm 0.2)$ for He. These data were calculated with an accessible volume map determined with a probe radius of 0.3 times the radius of the penetrant over a 250 ps simulation of PDMS without a penetrant particle. The error estimate is based on separate determinations over ten subsets of 25 ps each.

All these data are accumulated in Table III, and compared with experimental data. The solubility coefficient is
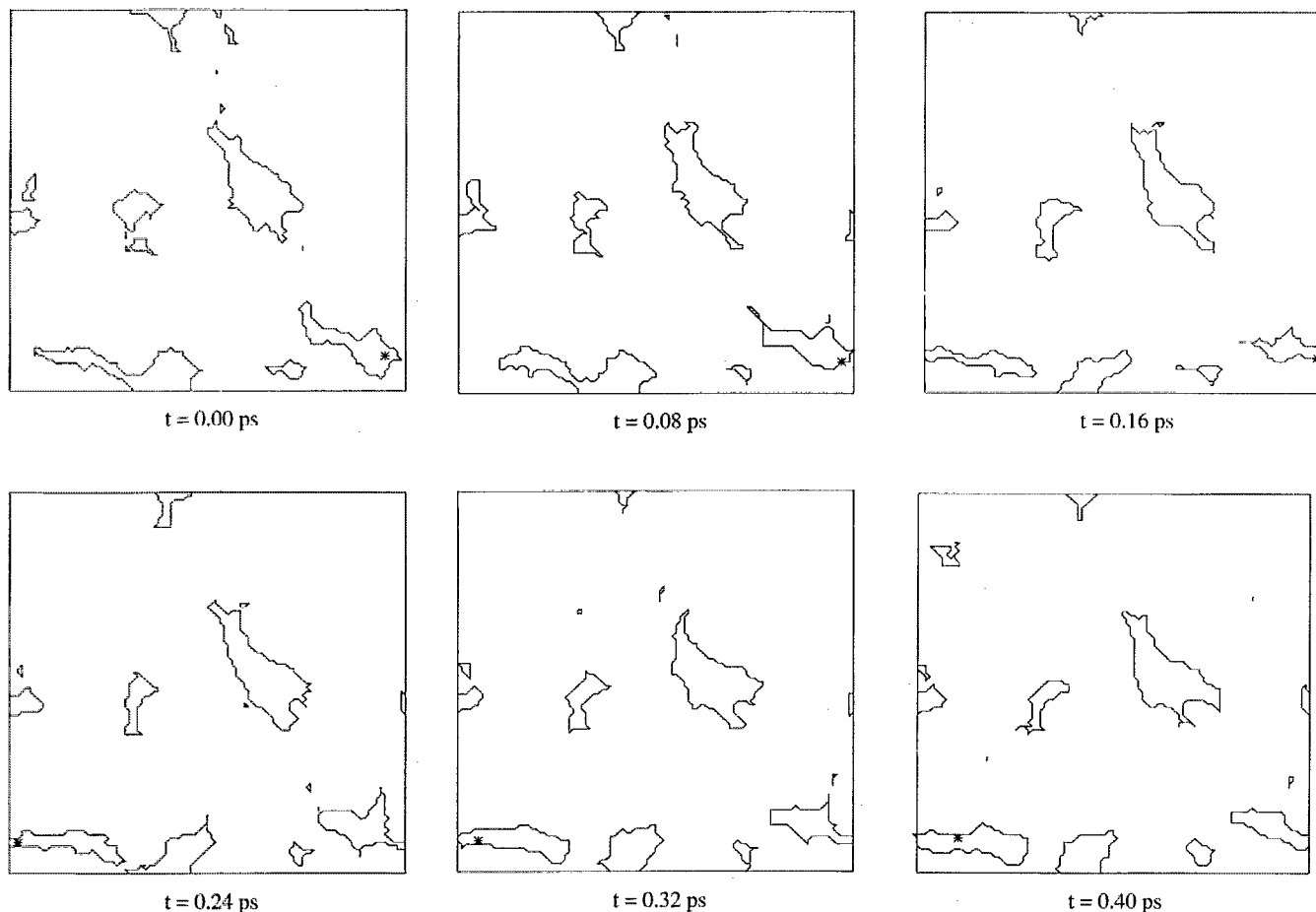
t = 0.00 ps   t = 0.08 ps   t = 0.16 ps

t = 0.24 ps   t = 0.32 ps   t = 0.40 ps

FIG. 5. A projection of the holes during the jump indicated by the arrow in Figs. 3 and 4. The star indicates the position of the CH_4 particle. The indicated times are relative to the first snapshot. Note that other holes, that do not contain a particle, are equally dynamic.
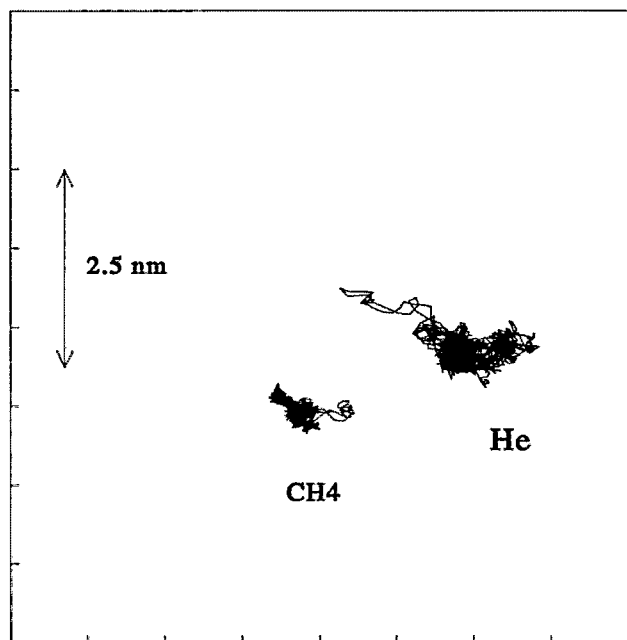

FIG. 6. Trajectories of CH_4 and He during a position restained simulation (PDMS frozen) of 250 ps each.
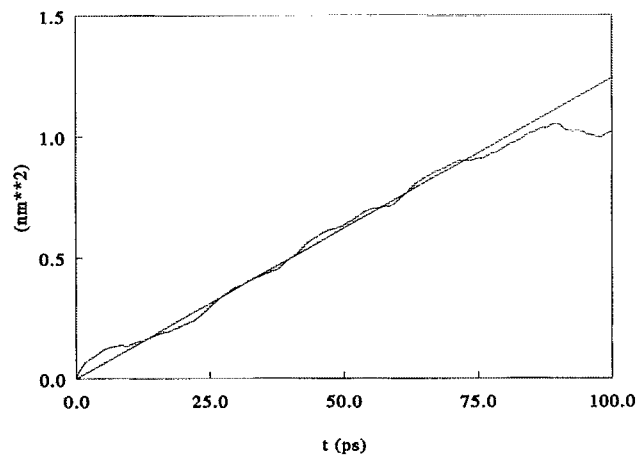

FIG. 7. Mean squared displacement curve of CH_4 in PDMS. The straight line is a weighted fit (weighted by t^{-2}) through the data points. The error in the slope is in the order of 40%. (All the 250 ps of the MSD are used for the fit, but only the significant part of the curve is shown.)

TABLE III. Comparison of experimental data (Refs. 15 and 16) and simulation results. Errors are given in parentheses.

	$D \times 10^9$ $(m^2 s^{-1})$	μ_{ex} $(kJ\ mol^{-1})$	S	$P \times 10^9$ $(m^2 s^{-1})$
CH_4 (expt.)	2.0	+ 1.5	0.56	1.11
CH_4 (This work)	2.1(0.8)	− 6.3(0.2)	12.5	26(7)
He (expt.)	10	+ 7.4	0.05	0.5
He (This work)	18(2)	+ 3.8(0.2)	0.22	3.9(0.6)

calculated from Eq. (2) from the experimental diffusion coefficient and permeability coefficient.

V. DISCUSSION

Our results have shown that the diffusion mechanism of small molecules as He and CH_4 in a polydimethylsiloxane matrix can be identified as a hopping between holes. For a helium atom the residence time per hole is so short that it nearly behaves as a freely diffusing particle; for methane the residence time is of the order of 25 ps, which considerably exceeds the transition time between holes. The mechanism by which the particle can move from one hole to another is clearly based on fluctuations of the polymer matrix which allow the transient opening of channels between holes. Thus the barrier for the motion of penetrant molecules between holes is decreased by the matrix fluctuations. The Boltzmann probability of crossing a barrier in a rigid polymer matrix is far too low to allow for diffusion, which is clearly shown by our rigid-matrix simulation.

It is clear from Table III that the computed absolute values of the chemical potential deviate from the corresponding experimental values by about 5–7 kJ/mol, but they do show the correct relative order of magnitude, i.e., the diffusion constant of He is larger than that of CH_4, but, due to the solubility part, the permeability coefficient of CH_4 is larger than that of He.

The discrepancy of 5–7 kJ/mol was also seen in a recent free energy calculation for gas absorption in amorphous polypropylene.[17] There the most likely source of discrepancy was given as the semicrystallinity of the experimental polypropylene. This argument, however, can not be applied to our PDMS system, which is (almost always) 100% amorphous. We attribute the discrepancy to the inaccuracy of the interaction potentials and/or to an overestimation of the polymer flexibility related to the limited chain length.

ACKNOWLEDGMENTS

[1] H. Takeuchi and K. Okazaki, J. Chem. Phys. 92, 5643 (1990).

[2] H. Takeuchi, J. Chem. Phys. 93, 2062 (1990).

[3] H. Takeuchi, J. Chem. Phys. 93, 4490 (1990).

[4] J. Sonnenburg, J. Gao, and J. W. Wiener, Macromolecules 23, 4653 (1990).

[5] F. Müller-Plathe, J. Chem. Phys. 94, 3192 (1991).

[6] F. Müller-Plathe, J. Chem. Phys. (submitted).

[7] Polymer Handbook, edited by J. Brandrup and E. H. Immergut (Wiley Interscience, New York, 1975).

[8] H. J. C. Berendsen and W. F. van Gunsteren, GROMOS Reference Manual (University of Groningen, Groningen, 1987).

[9] J-P. Ryckaert, G. Ciccotti, and H. J. C. Berendsen, J. Comp. Phys. 23, 327 (1977).

[10] R. W. Hockney and J. W. Eastwood, Computer Simulation Using Particles (McGraw-Hill, New York, 1981).

[11] H. J. C. Berendsen, J. P. M. Postma, W. F. van Gunsteren, and A. Di Nola, J. Chem. Phys. 81, 3684 (1984).

[12] J. H. R. Clarke and D. Brown, Mol. Sim. 3, 27 (1989).

[13] B. Widom, J. Chem. Phys. 39, 2802 (1963).

[14] G. L. Deitrick, L. E. Scriven, and H. T. Davis, J. Chem. Phys. 90, 2370 (1989).

[15] Y. Ichiraku, J. Membr. Sci. 34, 5 (1987).

[16] Data for Helium are estimates based on data for filled PDMS membranes. For example, from R. M. Barrer and H. T. Chio, J. Polym. Sci. C 10, 111 (1965).

[17] F. Müller-Plathe, Macromolecules 24, 6475 (1991).